Investigating a Null Test of the Einstein Equivalence Principle with Clocks at Different Solar Gravitational Potentials

Demetrios Matsakis
U.S. Naval Observatory (USNO)
Washington, DC 20392

***Abstract*—The Einstein Equivalence Principle (EEP) requires that clocks in free fall, when observed by other clocks in free fall, show no frequency variations. To some approximation, clocks on the surface of the Earth can be considered freely falling in the solar gravitational potential, and one would expect to find no frequency variations between the clocks as the Earth's rotation modulates the potential experienced by each clock. We investigate the attainable limits of a search for such a frequency variation using satellites, parameterized as a fraction of the expected differential gravitational redshift of a clock pair not in free fall. Under the most optimistic of assumptions, a 3-sigma limit to the EEP violation of 10^{-4} may be possible in the future, although the uncertainties we present are an order of magnitude higher, with an upper limit to an EEP violation of $<10^{-3}$.**

Keywords—General Relativity, Equivalence Principle, GPS, Precise Point Positioning, PPP, Two Way Satellite Time Transfer, TWSTT, TWSTFT

I. INTRODUCTION

Tests of Local Position Invariance (LPI), one of the tenets of the Einstein Equivalence Principle (EEP), typically rely on measurements of relativistic frequency shifts in clocks. The most common LPI tests are null measurements, looking for non-cancellation of gravitational and motional time dilation in the frequency comparison of two different types of clocks in the same local inertial frame. A fundamentally different null test can be carried out by looking for a non-cancellation of the relativistic frequency effects between two clocks at different gravitational potentials. This cancellation is routinely observed in GPS satellite clocks, and explained in [1] as due to the gravitational and Doppler effects having equal magnitude but opposite sign. Because the local inertial frame varies over the orbit, the authors of [2] argue for an approached based directly on the relativity of simultaneity,

Searches for EEP violations have tested relativity in many ways, often reporting upper limits in the range of 10^{-8}-2 10^{-13} [3]. The most comparable to our work with the solar-potential may be 1% results from Voyager and Galileo data [5,6], if not Gravity Probe A, whose measurement uncertainty was 2 10^{-4} (3-sigma) [7]. According to Schiff's conjecture, the validity of the Weak Equivalence Principle (WEP) necessarily implies the validity of the strong EEP, along with its two other components LPI and Local Lorenz Invariance [3, 4]. We search for a possible violation in the form of frequency differences between pairs of clocks that would vary diurnally, as the Earth's rotation modulates the solar potential experienced by each clock. The obstacle to carrying out such a test is the technology for frequency comparison of remote clocks. Our search for LPI violations employs time-transfer data obtained from both GPS and geostationary satellites; more precise comparisons via optical fibers are expected in the near future [8].

II. METHODOLOGY

In this work we report on two sets of data that were independently processed. One set is clock differences obtained via Two-Way Satellite Time Transfer (TWSTT) between the USNO in Washington, DC and its Alternate Master Clock (AMC) facility in Colorado Springs, Co. The other set is composed of clock differences from approximately eight years of GPS data from nine sites (Table 1), reduced with the Precise Point Positioning (PPP) technique by the International Bureau of Weights and Measures (BIPM) using standard products of the International GNSS Society (IGS), and we note that improvements to the PPP software may shortly become available for general use [9-11].

The interpretation of the GPS data in terms of general relativity (GR) requires an additional but plausible assumption that the IGS products for satellites on opposite sides of the Earth do not themselves contain an unmodelled LPI-violating component. No such assumption is needed for our TWSTT data, because the observations utilize a single transponder on their geostationary satellite and its effects are removed in the differencing between the forward and return paths. For PPP, an LPI-violation in the IGS satellite products would in general be expected to result in deviations stronger than on the Earth's surface, since laboratories on opposite sides of the Earth will be referenced to satellites whose differential effects are related to a maximum separation of eight Earth radii instead of two; however some of this amplification would be reduced since two non-equatorial sites with a longitude difference of even 180 degrees do observe some of the same satellites at the same

time. We have ignored this consideration in this work, but note that some IGS analysis centers use software that uses double double-differencing to compute orbits independently of the clocks; a comparison of these solutions with other solutions may also be sensitive to an EEP-violating effect.

In order to search for a diurnal frequency shift in ground clocks that would be in synchrony with the solar potential, we first create a many-day set of hourly-averaged frequency transfer data between pairs of sites. Daily solutions for the expected diurnals due to an EEP-violating parameter and its orthogonal "quadrature" parameter, that peaks six hours later, were obtained from daily fits over all data for which 24 hourly data points were still available after undergoing outlier-removal. The EEP-violating parameter was the frequency shift due to the gravitational potential expected from a clock at given latitude and longitude on the surface of the Earth at that time, using the following formulae:

$$\Delta f/f = -GM_{Sun}/(c^2 D_{Sun,}) \quad (1)$$

$$= -GM_{Sun} * r_{earth} * \cos(\theta) * \cos(\lambda)/(c^2 D^2_{Sun,0}) \quad (2)$$

$$= -4.0\ 10^{-13}\ \cos(\theta) * \cos(\lambda) * (D_{Sun,0}/D_{Sun})^2 \quad (3)$$

$$= -36\ \cos(\theta) * \cos(\lambda) * (D_{Sun,0}/D_{Sun})^2\ \text{ns/day} \quad (4)$$

where G is the gravitational constant, M_{Sun} is the solar mass, $D_{Sun,0}$ is one astronomical unit (nominal distance of the Sun from the center of the Earth), D_{Sun} is the distance of the Sun from the clock at the time of observation, r_{earth} is the nominal radius of the Earth, and θ is the angle of the Sun with respect to the meridian at the time of observation, and λ is the site latitude [12]. The Sun's declination was fixed over a day. The position and distance of the Sun were computed using the low-precision formulae provided in the Astronomical Almanac [13]. The peak frequency variation is doubled to 72 ns/day for clocks on opposite sides of the equator on the equinox.

Although neither of the sinusoidal parameters would correlate with an overall frequency average, a pre-fit average was removed to simplify the solution. As outlined in Appendix I, correlations between observations of site pairs that include a common site were taken into account using standard mathematical formulae that invoke the covariance matrix of the observations. For baselines (site pairs) that share a common site, the PPP data are correlated because the time transfer between any two sites is the difference between fitted values of the local clock vs. IGS time. For TWSTT, the correlation due to a common receive system is similar, because simultaneous observations with a common antenna have several common elements and the uncorrelated jitter is largely averaged out on hourly scales.

Solutions were carried out using two different methods for determining the covariances that involved common sites and were therefore expected to be nonzero. The first was to use the actual monthly-averaged correlations of the observation between frequencies determined over 12-hour intervals. The alternate method was to apply a covariance model with identical values for all observations. For TWSTT, values of +/-0.5 $(\text{ns/day})^2$ were assigned to each pair of baselines that included one common site; PPP covariances were given a value 1/4 of the TWSTT values. The autocorrelations (between identical baselines) had twice these values. These values can be described as "not untypical" of the much more varied correlations observed in the real data, however the correlations are used only to compute the daily global parameter solutions. Since the noise in the hourly averages exceeds the associated maser clocks' noise, some 3-day solutions were also generated by first averaging the data modulo one day in TWSTT data; however, the results did not significantly differ from the programmatically-simpler one-day solutions.

Once each day's batch of data was reduced, the daily parameter solutions were edited by removal of 3-sigma outliers (3%-7% of the data) and averaged into 10-day values, which were again edited to remove the very few 3-sigma outliers of the averages. The final values and statistics were determined by unweighted averaging of the ten-day averages.

Thermal and other effects unrelated to relativity that could cause a diurnal signature were ignored. Such diurnals are often observed in TWSTT; in many cases the time of peak amplitude varies quasi-linearly over long periods [14], and thus the diurnals would tend to be averaged out. For both techniques, any thermally-caused diurnals would be expected to correlate with the solar angle and the maximum/minimum thermal diurnal would be expected to occur several hours after noon/midnight. This signature would likely be split between the EEP-violating and the quadrature parameters.

We have also ignored the effects of solar tides, and the lunar potential. The rigidity of the Earth's response to the shifting potentials would result in a deviation from free-fall that we do not fully evaluate here. The maximum solar tide can be estimated as

$$r_{earth} * M_{Sun}/M_{Earth}/(D_{Sun,0}/r_{Earth})^3 = .16\ \text{m} \quad (5)$$

and its net frequency variation due to the Earth's field is

$$GM_{Earth}/(c^2 r^2_{Earth}) * (.16\text{m}) = 1.1 * 10^{-16}/\text{m} * .16\text{m} = 1.8\ 10^{-16} \quad (6)$$

and so the maximum effect as a fraction of the EEP-violating parameter would be $5\ 10^{-4}$.

Lunar effects would average out due to the 24.8 hours average time between meridian crossings, and that in any case their associated EEP-violation would be expected to be weaker by the solar/lunar mass ratio divided by their distance squared, or

$$(2.0*10^{30}\text{kg}/7.3*10^{22}\text{ kg}) / (1.5*10^8\text{ km}/3.8*10^5\text{ km})^2 = 420 \quad (7)$$

III. THE TWSTT AND THE PPP RESULTS

Figure 1 shows the fitted parameter values of the EEP-violating and its quadrature term in the TWSTT data, and Figure 2 shows the corresponding values in the PPP data. Although the mean values are near zero, the fitted parameters do not display a normal distribution and therefore the derived uncertainties can at best be considered upper limits. The derived average values can be considered to be a measure of the actual uncertainties, even though they would be statistically significant had the data displayed a truly normal distribution. This deviation from normality is by far strongest in the TWSTT solutions, and it is most likely due to the TWSTT data's strong diurnal signature.

PPP data can also have a diurnal signature. It is weaker, intermittent, variable in terms of daily peak times, and in general well below the noise level of the daily clock difference solutions. Some have been detected in our data using a Kalman filter similar to that employed to study TWSTT diurnals in [13]. IENG displayed diurnals often visible above the noise (Figure 3), and it was deleted from the analysis. Figures 4-5 show some examples of possible weak diurnals

Because the more recent data are of higher quality, a solution was also generated retaining only the data since MJD 56200. As shown in Table 2, this resulted in a lower standard deviation and lower mean.

-

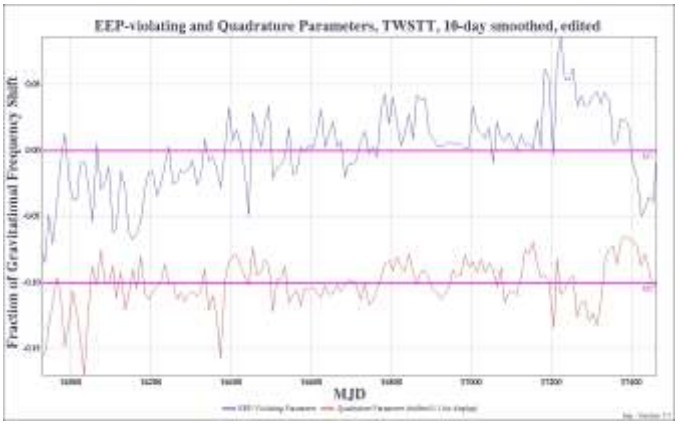

Figure 1. Ten-day averages of daily estimates of the EEP-violating and quadrature parameters, as determined by TWSTT, using the observed covariances to compute the daily solutions. Three-sigma outliers were removed at every step, and the quadrature curve was shifted by 0.1 for display purposes. The horizontal lines denote pre-shifted y=0, and the vertical scale is 0.05 per division.

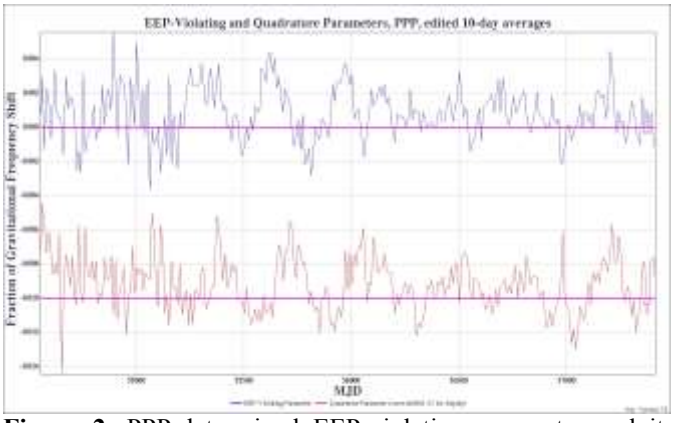

Figure 2. PPP-determined EEP-violating parameter and its quadrature counterparts, using the model covariances to compute the one-day solutions. Three-sigma outliers were removed at every step, and the quadrature parameter was shifted 0.01 for display purposes. The horizontal lines denote pre-shifted y=0, and the vertical scale is 0.002 (or 2 10^{-3}) per division.

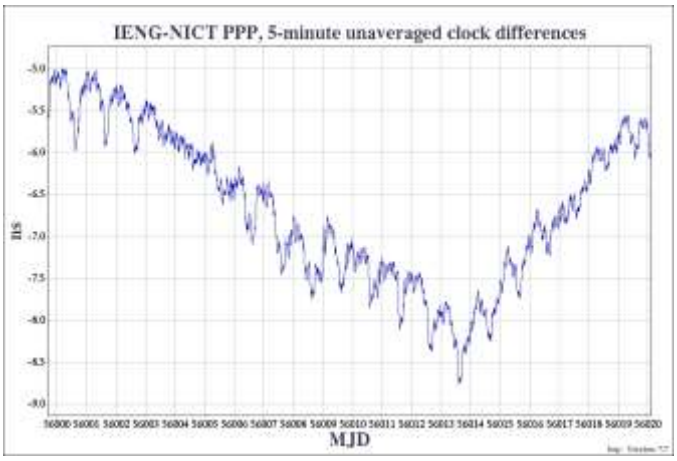

Figure 3. Diurnals in PPP data between IENG and NICT. Curve presents untreated 5-minute solutions as generated by the BIPM. This period shown is typical of the times when there are strong diurnals.

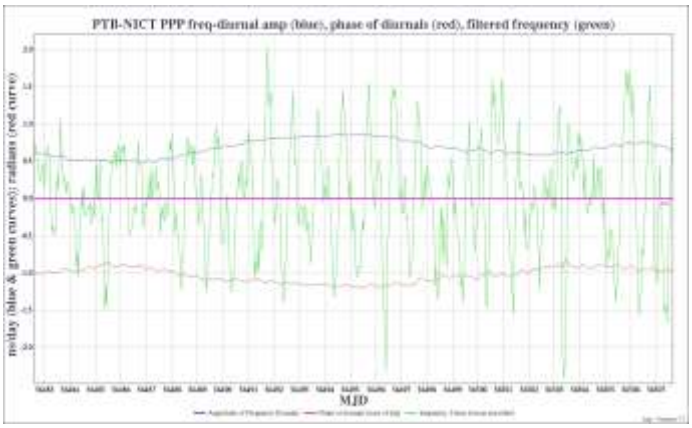

Figure 4. A period when a diurnal signature evident in PPP between receivers SEPB and PTBB. The blue curve is the Kalman-filter fitted amplitude of the diurnals, and the green curve is the data frequency difference smoothed over a 5-hour period with a boxcar filter. Both curves are in ns/day, and the red curve is the fitted phase of the diurnal in radians.

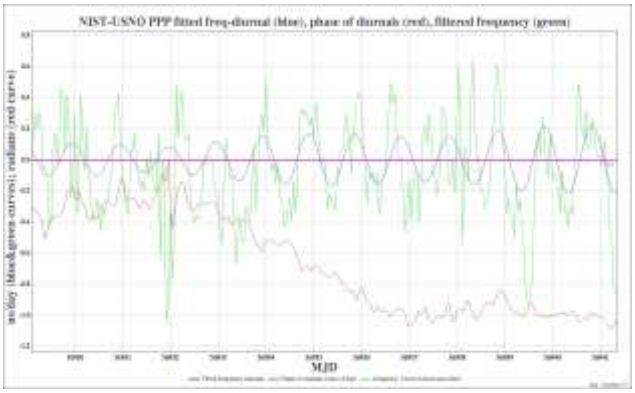

Figure 5. A period of possible diurnals in PPP between NIST and USNO. The curves depict the analogous quantities as in the previous figure.

IV. CONCLUSIONS AND FUTURE WORK

It is immediately evident in Table 2, and not surprising, that the greater signal to noise of PPP results in lower uncertainties and means. Since the uncertainties presented were computed using the standard deviations of the 10-day averages divided by the √N, the residual non-Gaussian nature of the smoothed data and the observation of unrelated (phase-varying) diurnal effects as well as unmodelled effects of solar tides imply that the uncertainties are underestimated. However, adding the assumption that IGS products are affected by an equivalent EEP-violation could result in lower uncertainties by a factor of up to four, while the interplay of solar tides with the Earth rigidity has not yet been modelled.

Future satellite-based time transfer data are expected to be significantly better. PPP improvements are expected because there will be improved software [as in 9-11], better clocks, more high-quality sites, and receive systems with less environmental and multipath sensitivity, along with data from multiple Global Navigation Satellite Systems (which themselves have different orbital parameters). It has been shown that the diurnal signature in TWSTT data can be largely reduced through the use of a software correlator [15], and if so this may enable future TWSTT comparisons using larger and more global arrays than employed in this work.

ACKNOWLEDGEMENTS

We thank Sean Urban for assistance with the astronomical computations, and Michael Efroimsky, Marshall Eubanks, Sergei Kopeikin, and Steven Peil for helpful discussions.

REFERENCES

[1] B. Hoffman, "Noon-Midnight Red Shift", Phys. Rev. 121, 1961, p 337

[2] N. Ashby and M. Weiss, "Why there is no noon-midnight shift in the GPS", http://arXiv [gr-qc]:1307.6525, 2013

[3] C. Will, "The Confrontation between General Relativity and Experiment", Living Rev. Relativity 17, 4, 2014

[4] S. Kopeikin, M. Efroimsky, and G. Kaplan, "Relativistic Celestial Mechanics of the Solar System", Wiley Press, 2011

[5] T.P. Krisher, J.D. Anderson, and J.K. Campbell, "Test of the gravitational redshift effect at Saturn", Phys. Rev. Lett, 64, 1332-1335,1990

[6] T.P. Krisher, D.D. Morabito, and J.D. Anderson, "The Galileo solar redshift experiment", Phys. Rev. Lett., 70, 2213-2216, 1993

[7] R.F.C.Vessot, M.W. Levine, E.M Mattison, E.L. Blomberg, T.E. Hoffman, G.U. Nystrom, B.F. Farrel, R. Decher, P.B. Eby, C.R. Baugher, J.W. Watts, D.L.Teuber, and F.O. Wills, "Test of relativistic gravitation with a space-born hydrogen maser", Phys. Rev. Lett. 5, 1980, pp. 2081-4.

[8] E-M Rasel, "Quantum tests of the Einstein Equivalence Principle on Ground and in Space, IFCS-EFTF, Denver, Co., 2015

[9] .J .Yao, I. Skakun, Z. Jiang, and J. Levine, "A detailed comparison of two continuous GPS carrier-phase time transfer techniques", Metrologia 52, 2015, pp. 666-676.

[10] J. Yao, J. Levine, and M. Weiss "Towards continuous GPS carrier-phase time transfer: eliminating the time discontinuity at an anomaly", J. Res. of NIST, 120, pp. 280-292, 2015.

[11] J. Yao, M. Weiss, C. Curry, and J. Levine, "GPS Jamming and GPS Carrier-Phase Time Transfer", these proceedings (ION-PTTI, 2016)

[12] E.E. Mamajek, A. Prsa, G. Torres, P. Harmanec, M. Asplund, P. D. Bennett, N. Capitaine, J. Christensen-Dalsgaard, E. Depagne, W. M. Folkner, M. Haberreiter, S. Hekker, J. L. Hilton, V. Kostov, D. W. Kurtz, J. Laskar, B. D. Mason, E. F. Milone, M. M. Montgomery, M. T. Richards, J. Schou, S. G. Stewart, "IAU 2015 Resolution B3 on Recommended Nominal Conversion Constants for Selected Solar and Planetary Properties", http://arXiv.org/abs/1510.07674, 2015

[13] The Astronomical Almanac is an official publication of the US Naval Observatory. Information is available on www.usno.navy.mil/usno/AA.

[14] D. Matsakis, "Characterizing the Diurnal Signature in Two Way Satellite Time Transfer (TWSTT) Data with a Kalman Filter", ION-PTTI, Monetery, Ca, 2016.

[15] Y.J. Huang, M. Fujieda, H Takiguchi, W-H Tseng, and H-W Tsao, "Stability improvement of an operational two-way satellite time and frequency transfer system", Metrologia 53, 2016, pp. 881-890

[16] The BIPM's receiver designations can be downloaded from this site: ftp://ftp2.bipm.org/pub/tai/publication/timelink/taippp, in a file named taippp_liste.xls

[17] The BIPM's acronyms for laboratories is downloadable as table 3 from here: http://www.bipm.org/en/bipm/tai/annual-report.html

[18] G.J.Beirman, Factorization methods for discrete sequential estimation, Academic Press, 1977, pp 47-49.

Table 1 GPS receivers employed in this work. All of the laboratories are listed as currently having their UTC realization based upon hydrogen masers, although some employed cesium standards initially. There were initially four labs in Europe, two in North America, and four in the Asian rim; however the data from one European lab were discarded. The last column is the average RMS of each day's 24 hourly frequencies, after removing a daily mean. The four NICT and two USNO units were employed sequentially. Note that all statistical stabilities are computed with reference to USN6, which was not initially available.

Receiver Acronym	Lab	Location	East Longitude	Latitude	Start Date	Stop Date	Daily Stability
[16]	[16]	City, Country	Degrees	Degrees	MJD	MJD	σ, ns/day, hourly pts
IENG (discarded)	IT	Torino, Italy	7.7	44.0	54552	57416	1.4
IMEJ	NIM	Beijing, China	116.9	39.9	56214	57416	1.4
NICT,SEPB,NC02,NC01	NICT	Tokyo, Japan	139.5	35.6	54552	56079	1.1
NIST	NIST	Boulder, Colorado, USA	-105.2	40.0	54552	57416	1.2
NM0C	NMIJ	Tsukaba, Japan	140.0	36.5	54552	57338	1.2
MIGT	MIKE	Espoo, Finland	24.65	60.1	55105	57296	1.2
PTBB	PTB	Braunschweig, Germany	10.5	52.3	54552	57416	1.2
ROAP	ROA	San Fernando, Spain	-6.0	36.5	54552	57416	1.3
TWTF	TW	Taipei, Taiwan	121.5	22.9	54552	57141	1.2
USN3	USNO	Washington, DC USA	-77.0	38.0	54552	56197	no overlap
USN6	USNO	Washington, DC USA	-77.0	38.0	56197	57416	Reference

Table 2 Summary of Derived Parameter Values, 10-day smoothed, edited, with final uncertainties determined from data scatter. TWSTT data were from Jan 2, 2012 through March 19, 2016. PPP data were from March 28, 2009 through January 29, 2015; the last two rows are based only on data since September 30, 2012.

Technique	# Days	Covariance Source	EEP-violating Parameter	Statistical Uncertainty	Quadrature Parameter
TWSTT	1538	Data	$-2.2\ 10^{-4}$	$\pm\ 2.4\ 10^{-3}$	$5.0\ 10^{-4}$
TWSTT	1538	Model	$1.4\ 10^{-3}$	$\pm\ 2.4\ 10^{-3}$	$5.5\ 10^{-3}$
PPP	2865	Data	$7.4\ 10^{-4}$	$\pm\ 1.1\ 10^{-4}$	$4.4\ 10^{-4}$
PPP	2865	Model	$7.9\ 10^{-4}$	$\pm\ 8.9\ 10^{-5}$	$7.8\ 10^{-4}$
PPP	1217	Data	$6.8\ 10^{-4}$	$\pm\ 1.1\ 10^{-4}$	$2.8\ 10^{-4}$
PPP	1217	Model	$6.1\ 10^{-4}$	$\pm\ 9.2\ 10^{-5}$	$4.4\ 10^{-4}$

Appendix I. Generalized Least Squares Parameter Fitting

Assume there are N pairs of sites (baselines) in the solution for a given day, and 24 hourly points available for each baseline in that solution. The average value of the 24 daily points from each baseline is subtracted out; in any case it is orthogonal to the two sinusoidal parameters fitted below.

Let S be the 24Nx24N covariance matrix of the observations. It can be determined by the monthly average of data, or set to a pre-determined value. Each baseline pair is composed of up to four sites, written as (A-B) and (C-D). If sites A, B, C, and D are four different sites, then the correlation is taken to be exactly zero. If sites A and C are identical, or if B and D are identical, then the correlation will be positive and related to the noise associated in the common site. If sites A and D are identical, or if sites B and C are identical, the correlation will be negative but again related to the noise of the common site. If site A is identical to site C site and site B is identical to site D, then the covariance is related to the root sum square (RSS) of the noise associated with site A and B. In all cases, it doesn't matter whether the "noise" is due to a variation of the clock associated with any given site or is due to the time transfer noise of that site's receive system. However, one criterion for the choice of sites was the quality of its clock.

We write $P=S^{-1}$, and define a solution design matrix A with 24*N rows and 2 columns. The elements of A are defined by dependence of the data on the EEP-violating and quadrature parameters. The two components of the parameter vector X are the EEP-violating term and its quadrature term. The data form a column vector Z, with 24*N components. The 24Nx24N covariance matrix of the observations, S, is computed using the geometrical considerations described in section II. Those elements of S whose corresponding baseline pairs are expected to have zero covariance are set to zero, the others are determined monthly using the observed covariances of mean-removed 12-hour frequencies.

The problem reduces to finding a 2-component column vector X, given data vector Z and design matrix A: $Z = A*X$, with known correlations S. It can be shown [16], that if $P=S^{-1}$, then X = final parameter values = $(A^T S^{-1}A)^{-1} *A^T S^{-1}*Z = (A^T PA)^{-1} *A^T*P*Z$, and the squared statistical uncertainties of the two parameters of X are the corresponding diagonal elements of $(A^T PA)^{-1}$.